Mechanics of Advanced Composite Structures 4 (2017) 211-223

Mechanics of Advanced Composite Structures
journal homepage: http://MACS.journals.semnan.ac.ir

Semnan University

Effects of Nanotube/Matrix Interface on Multi-Walled Carbon Nanotube Reinforced Polymer Mechanical Properties

K. Alasvand Zarasvand [a], H. Golestanian [b,c*]

[a] *Department of Mechancical Engineering, Shahrekord University, Shahrekord, Iran*
[b] *Faculty of Engineering, Shahrekord University, Shahrekord, Iran*
[c] *Nanotechnology Research Center, Shahrekord University, Shahrekord, Iran*

PAPER INFO

Paper history:
Received 2016-12-17
Revised 2017-01-03
Accepted 2017-02-08

Keywords:
Multi-Walled Carbon Nanotube
Nanocomposite
Compressive Properties
Experimental
Connector Constraint

ABSTRACT

In this paper, experimental and Finite Element Methods have been used to determine mechanical properties of nanocomposites. Standard tensile and compression samples with 0.0, 0.15, 0.25, 0.35, 0.45, and 0.55 weight fraction of Multi-Walled Carbon Nanotube (MWCNT) were prepared and tested. Nanotube weight fraction was varied to investigate the effects of nanotube weight fraction on nanocomposite mechanical properties. Mechanical properties such as: modulus of elasticity, yield strength, ultimate tensile strength, and fracture strain were determined experimentally. Experimental results showed that incorporation of carbon nanotubes improves modulus of elasticity, and yield and ultimate strengths of the epoxy resin under tension and compression. Results also showed that fracture strain decreases drastically with increasing nanotube weight fraction. Field Emission Scanning Electron Microscope (FESEM) was used to obtain images of the samples' fracture surfaces. These images showed a good MWCNT dispersion in the matrix. Also, numerical simulations were conducted in Abaqus software. In these simulations, the effects of the interface between individual nanotubes and the outer nanotube and matrix were investigated. Two different models were used for these interfaces. Connector constraints were used in the first model and thin shells in the second model. The connector model predicted lower mechanical properties compared to the thin shell interface model. Finally, experimental and numerical results were compared and a good correlation was observed between the results.

DOI: 10.22075/MACS.2017.1799.1093

1. Introduction

Carbon Nanotubes (CNTs) are known for their very remarkable electronic, thermal, optical, mechanical, and chemical properties [1, 2]. These properties imply potential application of CNTs as reinforcement in polymer nanocomposites [3, 4]. For these reasons CNT reinforced polymers have gained much attention among researchers in recent years [5, 6]. The significant enhancements in polymer/CNT composite mechanical properties are generally related to the degree of CNT dispersion, impregnation, and interfacial adhesion between CNT and matrix [5]. Because of their high adhesion, low weight, and good chemical resistance, epoxy-based composite materials are being increasingly used as structural components in aerospace and automotive industries. However, the relatively weak mechanical properties of epoxy have prevented its application in components that demand high mechanical strength and stability. The physical properties of cured epoxy resins depend on their structure, their curing extent, and their curing time and temperature. For this reason, it is necessary to know and to understand the relationship between the network structure and the final properties of the material, to obtain resins suitable for high performance applications [7, 8]. The reinforcement efficiency of CNT in a matrix depends on content of fillers, dispersion morphology, type of bonding with the surrounding polymer, aspect ratio, and waviness of nanotubes [9]. An appropriate level of CNT dispersion is often achieved through severe sonication or shear mixing in a three rolls process. Otherwise, aggregation of

* Corresponding author. Tel.: +98-38-34424438; Fax: +98-38-34424438

E-mail address: golestanian@eng.sku.ac.ir

CNTs creates defect sites which weaken the nanocomposite mechanical properties [9].

Gkikas et al. discussed the effect of dispersion conditions on thermal and mechanical properties and toughness of multi-walled carbon nanotube (MWCNT), reinforced epoxy nanocomposites [5]. These investigators showed that best results were obtained with 2h of sonication and 50% sonication amplitude to achieve appropriate dispersion level of CNTs in epoxy matrices without destroying the CNT's structure. Srivastava, investigated the effects of MWCNTs weight fraction on Young's modulus and tensile and compressive strengths of polymer-based nanocomposites [7]. The results of this investigation indicated that the mechanical properties of epoxy resin were improved with the addition of CNT fillers. Rahmanian et al. determined mechanical properties of three-phase nanocomposites experimentally [9]. Their samples consisted of epoxy resin reinforced with short carbon fibers and MWCNT fibers. Montazeri et al. investigated the mechanical properties of epoxy reinforced with MWCNTs [10]. These investigators examined the effect of increasing the weight fraction, and surface modification of MWCNTs on mechanical properties of nanocomposites. Ayatollahi et al. studied the effects of MWCNT aspect ratio on the mechanical and electrical properties of epoxy/MWCNT nanocomposites [11]. They found that the MWCNT aspect ratio has a significant effect on both electrical and mechanical properties of nanocomposites with significantly better properties with MWCNTs of smaller diameter. Xu et al. also determined properties of nanocomposites experimentally [12]. Their results showed that the improvement in mechanical properties is negligible. They claimed that a significant improvement in mechanical properties of nanocomposites could not be achieved, even with the use of surfactants. Fereidoon et al. studied the effect of functionalizing MWCNTs in improving mechanical properties of epoxy resins [13]. Their results showed that, existence of nano-filler has positive effects on mechanical properties of nanocomposites. Also, functionalized nano-filler with acid and amino agent showed improvement in epoxy mechanical properties. Maa et al. investigated the effects of CNT volume fraction on nanocomposite mechanical properties experimentally [14]. They observed an improvement in nanocomposite mechanical properties with an addition of CNTs to epoxy resin. Montazeri and Chitsazzade studied the effect of sonication parameters on the mechanical properties of MWCNTs/epoxy composites [15]. Their results indicated that with increase in the sonication time, there is an initial increase in Young's modulus values followed by a drop in values at longer sonication times. Chen et al. performed a study on the cryogenic mechanical properties of MWCNT reinforced epoxy nanocomposites [16]. Their samples were prepared by adding MWCNTs to diglycidyl ether of bisphenol-F epoxy via the ultrasonic technique. Ma et al. investigated compressive properties of epoxy with different CNTs contents at quasi-static and high strain rate loadings [17]. Their results indicated that the compressive failure stress of composites with various CNT contents was increased with strain rate and CNT content. Ghosh et al. investigated the influence of ultrasonic dual mixing on thermal and tensile properties of MWCNTs-epoxy nanocomposite [18]. Their results showed that the thermal stability, tensile strength, and toughness of the epoxy improve with MWCNT addition up to 1.5 wt. %.

Joshi et al. discussed load transfer in MWCNT composites under tension and compression loading conditions [19]. Their results indicated that with the addition of MWCNTs in a matrix at volume fraction of 5.1%, the stiffness of the composite increased by 46% in compressive loading and 14.9% in tensile loading. Also, Joshi et al. reported elastic response of MWCNT reinforced composite for different interphase properties between matrix and MWCNTs [20]. These investigators showed that improvement in mechanical properties of a soft matrix has strong dependence on interphase thickness. Giannopoulos et al. described a micromechanical finite element approach for the estimation of the effective Young's modulus of single-walled carbon nanotube (SWCNT) reinforced composites [21]. Also, these researchers investigated the effect of the interface on the performance of the composite for various CNT volume fractions. Weidt et al. predicted the macroscopic finite strain compressive behavior of CNT/epoxy nanocomposites at quasi-static and high strain-rates using 2D and 3D Representative Volume Element (RVE) approaches [22]. Their results showed that the nanocomposite nonlinear compressive stress–strain response cannot be accurately captured using 2D RVEs compared to 3D RVEs. Zuberi et al. estimated the mechanical properties of SWCNT reinforced epoxy composite through finite element modeling [23]. They used two approaches: non-bonded interactions and perfect bonding model to simulate interface regions. Shokrieh et al. studied tensile behavior of embedded CNTs in a polymer matrix in presence of van der Waals interaction as the interphase region [24]. Their results indicated that improvement in the Young's modulus of CNT-composite is negligible for CNT lengths smaller than 100 nm and saturation takes place for CNT lengths in the order of 10 μm. Mohammadpour et al. presented a finite element model for predicting the mechanical behavior of polypropylene (PP) reinforced with CNTs at large deformation scale [25]. Golestanian and Shojaei used finite element method to in-

vestigate the effects of interface strength on effective nanocomposite mechanical properties [26]. Their results indicated that longitudinal modulus of nanocomposite increases with interface strength.

As shown by the presented literature review, many researchers have determined mechanical properties of nanocomposites using experimental and numerical methods. First, these investigations have been limited to the determination of effective mechanical properties of nanocomposites under tensile loading conditions. Compressive mechanical properties have rarely been investigated using experimental methods. Second, compressive effective mechanical properties of nanocomposites with three layer MWCNTs have not been studied numerically. In this paper, experimental and numerical methods have been used to determine mechanical properties of epoxy-based nanocomposites reinforced with MWCNTs. Standard nanocomposite samples containing different amounts of carbon nanotube were prepared and were tested under tensile and compressive loads. Mechanical properties such as: modulus of elasticity, yield strength, ultimate strength, and fracture strain were determined experimentally. Field Emission Scanning Electron Microscope (FESEM) was used to obtain images of specimen fracture surfaces and to asses MWCNTs dispersion in the matrix. In addition, numerical simulations of nanocomposites were conducted in Abaqus finite element software. In these simulations two different models were made to investigate the effects of the interface strength on nanocomposite mechanical properties. In the first model, an interface consisting of a series of hinge and axial-universal connector constraints were used. In the second, a finite element model, an interface consisting of a thin shell was used between the MWCNTs layers and the matrix. Note that the connector constraint model has been used for the first time to estimate effective tensile and compressive Young's moduli with better accuracy in comparison with models presented in other investigations. The interface strength was assumed to be lower than the matrix strength because of imperfect bonding between the two. The stiffnesses of the connectors and thin shell interface were varied between 0.2 and 1.89 GPa (perfect bonding). Finally, experimental and numerical simulation results were compared.

2. Experimental

2.1. Materials

Epoxy resin was selected as the matrix material because it is widely used in the composite industry for its good stiffness, strength, chemical resistance, and dimensional stability [9, 27].

Epoxy FK20, which is a bisphenol-A resin, and the corresponding hardener were used in this investigation. Two parts of epoxy is mixed with one part of the hardener, by weight. MWCNTs, obtained from US Research Nanomaterials Inc. (US-NANO), are used as the reinforcement. Carbon nanotube specifications were obtained from the supplier and are listed in Table 1.

2.2. Specimen Preparation

Tensile and compression test specimens were prepared by adding the required amount of MWCNTs (0, 0.15, 0.25, 0.35, 0.45 and 0.55 weight %) to the monomer. Next, this mixture was stirred using a mechanical stirrer at a speed of 1000 rpm for 60 minutes. To homogenize the dispersion and break any possible agglomerations of the carbon nanotubes, the mixture was sonicated for 60 minutes using an ultrasonic bath. Iced water bath was used to keep down the temperature of the solution during the sonication process. The sonication process was paused for 3 minutes after every 10 minutes of sonication. Next, the solution was placed under vacuum for 15 minutes to remove any trapped air. After degassing, the hardener was added and the solution was stirred gently for 5 minutes. Then this solution was placed under vacuum for 10 minutes again. Finally, the nanocomposite solution was poured into the mold and cured at 85°C for three hours followed by a post cure of one hour at 120°C.

2.3. Mechanical Property Characterization

Mechanical properties of pure resin and nanocomposites were determined through the use of tensile and compression tests. Tensile and compressive specimens were prepared and were tested according to D638-IV and D695 ASTM standards [28, 29], respectively. A picture of some samples of the standard specimens are shown in Fig. 1. Also, a hypothetical arrangement of the CNTs in the matrix is shown in this figure at two scales. Four tensile test specimens with dimensions 115 mm long × 12.7 mm wide and 3 mm thick in a dog-bone shape were each tested for CNT weight fraction. In addition, four 9 mm long and 8.5 mm diameter cylindrical compression test specimens were prepared and tested at each MWCNT weight fraction. Thus, a total of 48 tests were conducted. Santam universal testing machine STM-20 with a 20 kN load cell was used to perform these tests. Tensile and compression tests were performed at speeds of 10 mm/min and 0.5 mm/min, respectively. One of the pure resin samples after tensile testing can be seen in Fig. 2.

Table 1. MWCNT specifications

Young Modulus	Length	Inner Diameter	Outer Diameter
1000 GPa	30 μm	$3-5(nm)$	$5-15\ (nm)$

2.4. FESEM studies

To investigate MWCNTs dispersion in the epoxy matrix, a FESEM (model Mira 3-XMU), powered by second-generation EDS microanalysis, was used. Because of the nonconductive property of the epoxy polymer, fracture surfaces were coated with a layer of gold before taking the images.

3. Numerical Characterization

In this paper, mechanical properties of MWCNT reinforced epoxy resin were estimated using Finite Element (FE) simulations. In the FE models, to simulate MWCNTs, the three walled carbon nanotubes were embedded into a Representative Volume Element (RVE). To consider the effect of van der Waals bonding between carbon nanotube layers, each layer of the CNT is connected to the adjacent layer using axial and torsional connector constraints. Three dimensional model of three walled carbon nanotube embedded in square RVE with connector constraint interphase is shown in Fig. 3. Also, dimensions of MWCNT used in these models are shown in Fig. 4. Note that the lengths of MWCNT and RVE used in these simulations are 100 nm and 200 nm, respectively. In this investigation, a linear analysis has been performed to obtain effective mechanical properties of nanocomposites. These models are simulated using C3D8R elements to decrease the computational costs. The two effective axial and lateral Young's moduli ($\boldsymbol{E_z}$, $\boldsymbol{E_x}$) are determined numerically. The general 3-D strain–stress relation relating the normal stresses (σ_x, σ_y, σ_z) and strains (ε_x, ε_y, ε_z) for a transversely isotropic material can be written as [26, 30]:

$$\begin{Bmatrix}\varepsilon_x\\ \varepsilon_y\\ \varepsilon_z\end{Bmatrix}=\begin{bmatrix}\frac{1}{E_x} & \frac{-v_{xy}}{E_x} & \frac{-v_{zx}}{E_z}\\ \frac{-v_{xy}}{E_x} & \frac{1}{E_x} & \frac{-v_{zx}}{E_z}\\ \frac{-v_{zx}}{E_z} & \frac{-v_{zx}}{E_z} & \frac{1}{E_z}\end{bmatrix}\begin{Bmatrix}\sigma_x\\ \sigma_y\\ \sigma_z\end{Bmatrix} \quad (1)$$

To determine axial and lateral elastic moduli ($\boldsymbol{E_z}$, $\boldsymbol{E_x}$), two load cases were applied on the square RVE. In the first load case, shown in Fig. 4(b), the RVE is subjected to an arbitrary axial elongation. In the second load case, shown in Fig. 4(c), the RVE is subjected to a known lateral distributed load. These load cases and the corresponding formulations are discussed in the following sections.

3.1. Uniaxial Loading Case

In this case, the stress and strain components on the lateral surface are given by [26];

$\sigma_x=\sigma_y=0, \varepsilon_z=\frac{\Delta L}{L}, \varepsilon_x=\frac{\Delta x}{a}$ along $x=\pm a$, and;

$\varepsilon_y=\frac{\Delta y}{a}$ along $y=\pm a$

where Δa is the change of the cross section length, a, under the elongation ΔL applied in the z-direction. Integrating and averaging the third equation in Equation (1) on the plane $Z=L/2$, we obtain [26];

$$E_z=\frac{\sigma_{ave}}{\varepsilon_z}=\frac{L}{\Delta L}\sigma_{ave} \quad (2)$$

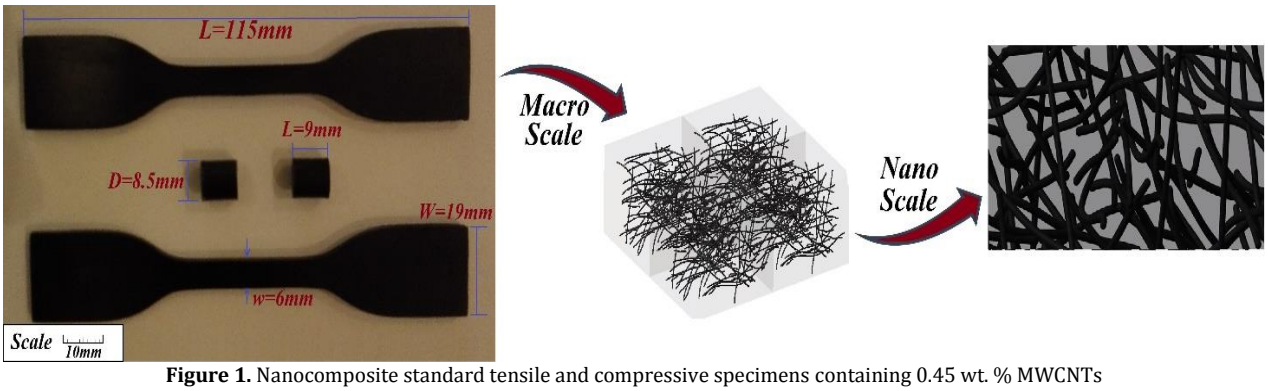

Figure 1. Nanocomposite standard tensile and compressive specimens containing 0.45 wt. % MWCNTs

Figure 2. Picture of a pure resin sample after tensile testing

where $\boldsymbol{\sigma_{ave}}$ is the average value of stress in the *z*-direction, given by [26];

$$\sigma_{ave} = \frac{1}{A}\int_A \sigma_z\left(x, y, \frac{L}{2}\right) dxdy \tag{3}$$

where *A* is the RVE cross sectional area. The value of $\boldsymbol{\sigma_{ave}}$ is evaluated by averaging stresses in the *z*-direction over all elements in the cross section at *L/2*. Using one of the relations in equation (1), together with the value of $\boldsymbol{E_z}$ found from equation (2), along *x=±a* we have [26];

$$\varepsilon_x = \frac{-v_{zx}}{E_z}\sigma_z = -v_{zx}\frac{\Delta L}{L} = \frac{\Delta a}{a} \tag{4}$$

Thus, we can obtain an expression for the Poisson's ratio as follows [26];

$$v_{zx} = -\left(\frac{\Delta a}{a}\right)/\left(\frac{\Delta L}{L}\right) \tag{5}$$

Equations (2) and (3) can be applied to estimate the effective Young's modulus $\boldsymbol{E_z}$ and Poisson's ratio $\boldsymbol{v_{zx}}$, once the contraction *Δa* and the average stress, $\boldsymbol{\sigma_{ave}}$, in case (*a*) are obtained [26].

3.2. Square RVE under a Lateral Uniform Load

In this load case, Fig. 4(c), the square RVE is loaded with a uniformly distributed tensile load, *p*, in one of the lateral directions, in this example the *y*-direction. The RVE is constrained in the *z*-direction. Thus, the 3D strain–stress relations for normal components in Equation (1) are reduced to [26];

$$\begin{Bmatrix}\varepsilon_x\\ \varepsilon_y\end{Bmatrix} = \begin{bmatrix}\frac{1}{E_x}-\frac{v_{zx}^2}{E_z} & -\frac{v_{xy}}{E_x}-\frac{v_{zx}^2}{E_z}\\ -\frac{v_{xy}}{E_x}-\frac{v_{zx}^2}{E_z} & \frac{1}{E_x}-\frac{v_{zx}^2}{E_z}\end{bmatrix}\begin{Bmatrix}\sigma_x\\ \sigma_y\end{Bmatrix} \tag{6}$$

For the corresponding elasticity model we have the following results for the normal stress and strain components at a point on the lateral surfaces:

$\sigma_x = 0, \sigma_y = P, \varepsilon_y = \frac{\Delta y}{a}$ along $y = \pm a$

Where *Δy* is the change of dimension in the *y*-direction. Applying the second part of equation (6) for points along *y=±a* together with the above conditions, we obtain [26];

$$\varepsilon_y = \left(\frac{1}{E_x}-\frac{v_{zx}^2}{E_z}\right)p = \frac{\Delta y}{a} \tag{7}$$

Solving equation (7) gives the effective Young's modulus in the transverse direction, *x*–*y* plane as in Fig. 4(c);

$$E_x = E_y = \frac{1}{\left(\frac{\Delta y}{Pa}+\frac{v_{zx}^2}{E_z}\right)} \tag{8}$$

The results of axial elongation loading case are used in equation (8) for $\boldsymbol{E_z}$ and $\boldsymbol{v_{zx}}$. Once the change in dimension, Δ*y*, is determined for the square RVE from a finite element analysis, $\boldsymbol{E_x}$ can be computed from equation (8) [26].

4. Results and Discussion

Tensile and compression tests were performed on six different samples with 0, 0.15, 0.25, 0.35, 0.45 and 0.55 nanotube weight fractions, as stated above. As nanotube weight fraction increases, CNT agglomeration becomes a problem. To achieve a suitable dispersion and a better verification of numerical method, low contents of MWCNTs up to 0.55 weight fractions were used in this investigation. In addition, two different numerical models were created to determine the nanocomposite mechanical properties at each CNT weight fraction. The results of these investigations are presented in this section, separately.

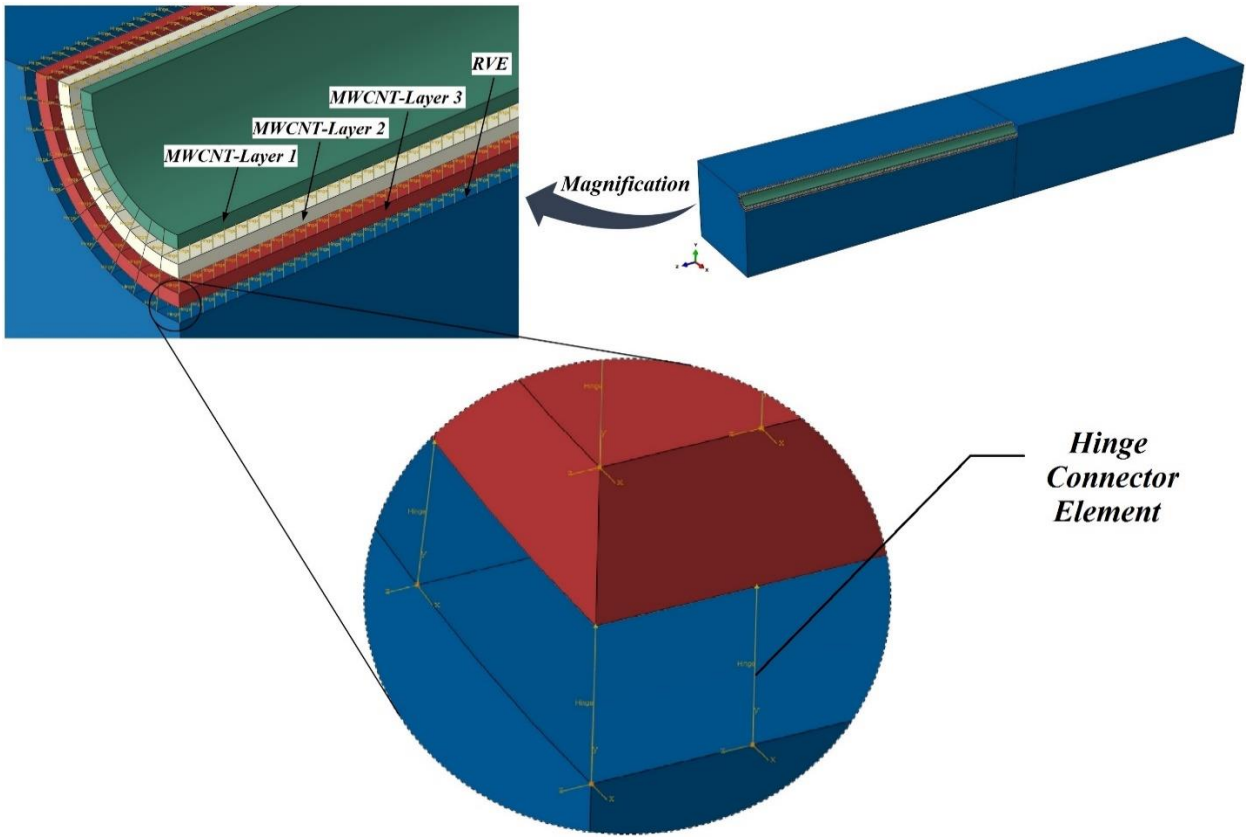

Figure 3. Three dimensional model magnification of the three walled carbon nanotube embedded in square RVE (the magnification shows the connectors)

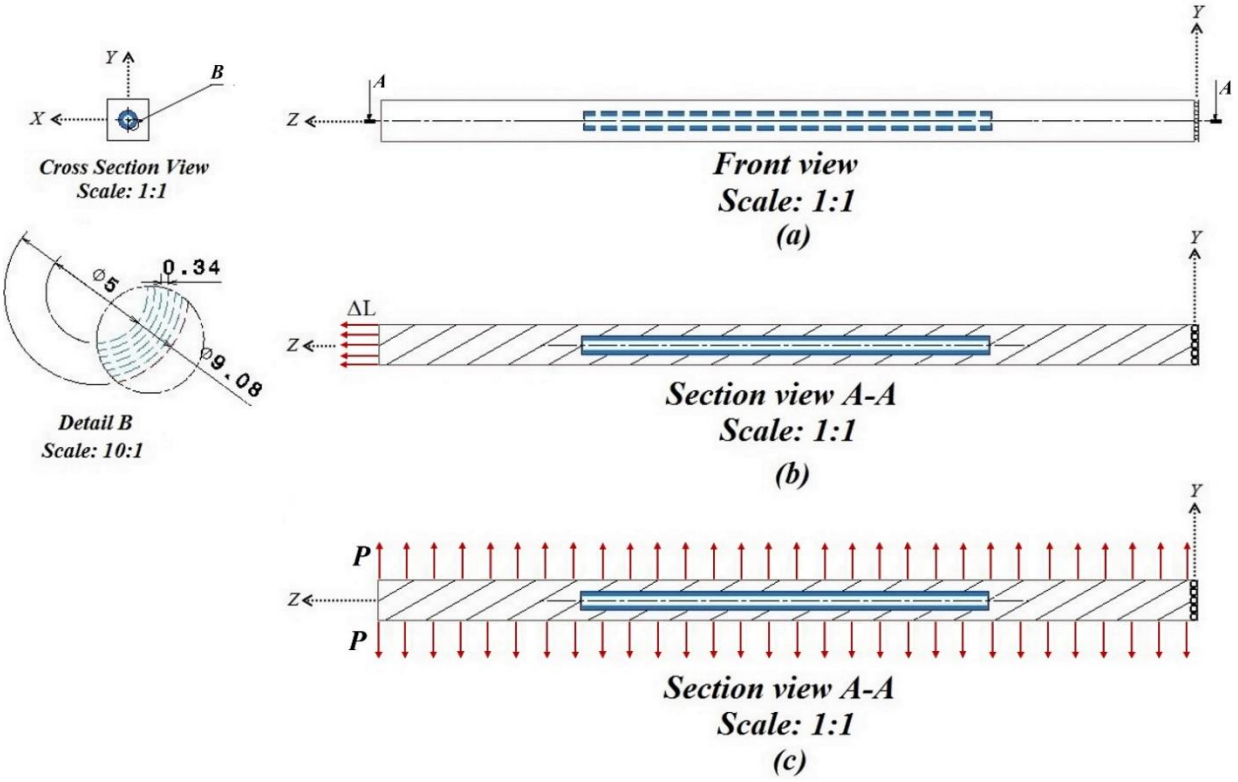

Figure 4. Two dimensional schematic of nanocomposite under axial and lateral loading cases

4.1. Experimental Characterization Results

Tensile test results of the six sample cases are compared in Fig. 5(a). Nanocomposite tensile properties are listed in Table 2. The properties listed in this table are the average of several test results. As can be seen in Table 2, yield strength and ultimate tensile strength of the nanocomposite both increase with reinforcement weight fraction. The results indicate that with the addition of 0.55 weight percentage of MWCNTs, yield strength and ultimate tensile strength increase 50% and 29.7%, respectively. In comparison, ultimate tensile strength obtained by Montazeri et al. [10] shows an increase of only 8% with the addition of 0.5 wt. % MWCNT. Note in Table 2 that tensile test results indicate a meaningful increase in resin modulus of elasticity, yield strength, and ultimate tensile strength with CNT weight fraction. Fracture strain, however, decreases drastically with CNT weight fraction. This suggests a much more brittle behavior of the epoxy resin with the addition of the MWCNTs.

In this study, six different samples were prepared and tested under compression. Compression test results of each of these six sample cases are compared in Fig. 5(b). Nanocomposite compressive properties are listed in Table 3. As can be seen in Table 3, yield strength and compressive strength of the nanocomposite increase with reinforcement weight fraction. Compressive strength presented by Srivastava [7] showed an increase of 13% with the addition of 0.5 wt. % MWCNTs. Further results of this investigation indicated that addition of 0.55 weight % of MWCNTs, yield strength and compressive strength increased by 16.7% and 20.2%, respectively. Note in Table 3 that compressive modulus of elasticity initially increases with the addition of carbon nanotubes up to 0.45 % weight fraction of the CNTs. At higher CNT weight fractions, nanocomposite compressive modulus of elasticity decreases slightly. This could be due to a possible agglomeration of carbon nanotubes in epoxy resin at high CNT weight fractions. Standard deviation is used to show the variation of nanocomposite mechanical property values about their arithmetic mean in Tables 2 and 3. It is observed that the variations in the data for each MWCNTs weight fraction are acceptable.

4.2. FESEM analysis

Field Emission Scanning Electron Microscope (FESEM) was used to obtain images of the sample fracture surfaces. This was done to investigate the MWCNT dispersion in the matrix with high resolution. Fig. 6 presents a nanocomposite fracture surface of the 0.45 wt. % MWCNT nanocomposite. Images in Figs. 6(a), 6(b), and 6(c) are taken from the same sample, but at 15,000x, 75,000x, and 75,000x magnifications, respectively. Note that the MWCNTs are well dispersed in the matrix. Broken MWCNTs and pull outs are also observed in these images. In addition, CNT diameters have been measured and given in the images. Note in these figures that good nanotube dispersion was achieved through the use of sonication and mixing processes. As a result, the level of MWCNT dispersion in this investigation shows better distribution in comparison with investigations presented by Srivastava [7] and Montazeri et al. [10]. As evidence, many CNTs show pull outs from the matrix in SEM images obtained by Srivastava [7]. The fact that CNT pullout is observed in these micrographs suggests that interfacial bonding between the CNTs and the matrix was not perfect. The presence of CNT pull outs further suggests the need to investigate interfacial strength effects on nanocomposite mechanical properties. Understanding this phenomenon is one of the main goals in this investigation.

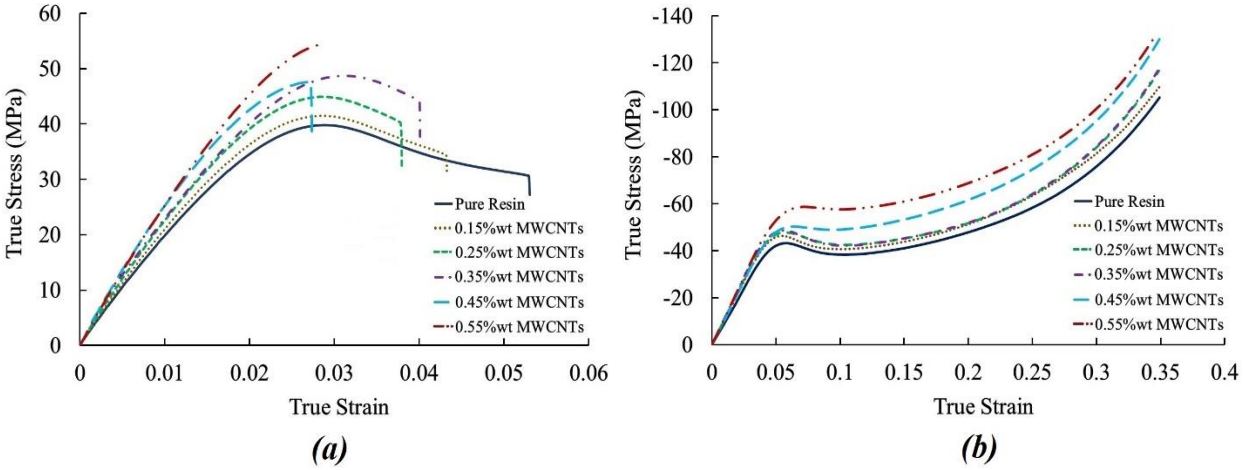

Figure 5. Stress-strain diagrams of the six samples under investigation: (a) tensile, (b) compressive

Table 2. Experimental mechanical properties of pure resin and the five nanocomposites under tensile loading

Tensile mechanical properties	Pure resin	0.15 wt.%	0.25 wt.%	0.35 wt.%	0.45 wt.%	0.55 wt.%
Modulus of elasticity (MPa)	1880.7±42	1932.6±70	2077.3±52	2137.6±86	2230.4±34	2268.1±110
Yield strength (MPa)	16.15±0.35	17.55±0.63	17.91±0.47	18.55±0.76	19.24±0.29	20.62±1.0
Ultimate Tensile strength (MPa)	39.77±0.88	41.44±1.5	44.82±1.2	47.54±1.7	48.11±0.63	51.03±2.2
Fracture strain	0.053±0.002	0.047±0.002	0.044±0.001	0.041±0.002	0.041±0.001	0.030±0.001

Table 3. Experimental mechanical properties of pure resin and the five nanocomposites under Compession Loading

Compressive mechanical properties	Pure resin	0.15 wt.%	0.25 wt.%	0.35 wt.%	0.45 wt.%	0.55 wt.%
Modulus of elasticity (MPa)	897.15±35	930.02±54	950.23±38	956.94±44	988.16±64	962.00±65
Upper Yield strength (MPa)	43.2±1.53	45.3±2.6	48.1±2.0	48.5±1.95	50.6±3.1	51.9±2.9
Compressive strength (MPa)	105.3±3.9	109.7±5.4	116.6±4.6	117±5.1	129.9±6.5	132±5.7

4.3. Numerical Results Validation

To validate the numerical simulation results, nanocomposite longitudinal modulus determined using the two interface models are compared with experimental measurements in Fig. 7. Note that nanocomposite longitudinal modulus increases with CNT weight fraction in all cases, as expected. Note also that the difference between the numerical and experimental results is less than 5% in all cases. Further, note that the connector constraint interface model predicts lower modulus of elasticity than the thin shell interphase model. It is also observed that the results of the thin shell model are closer to the experimental results from tensile loading.

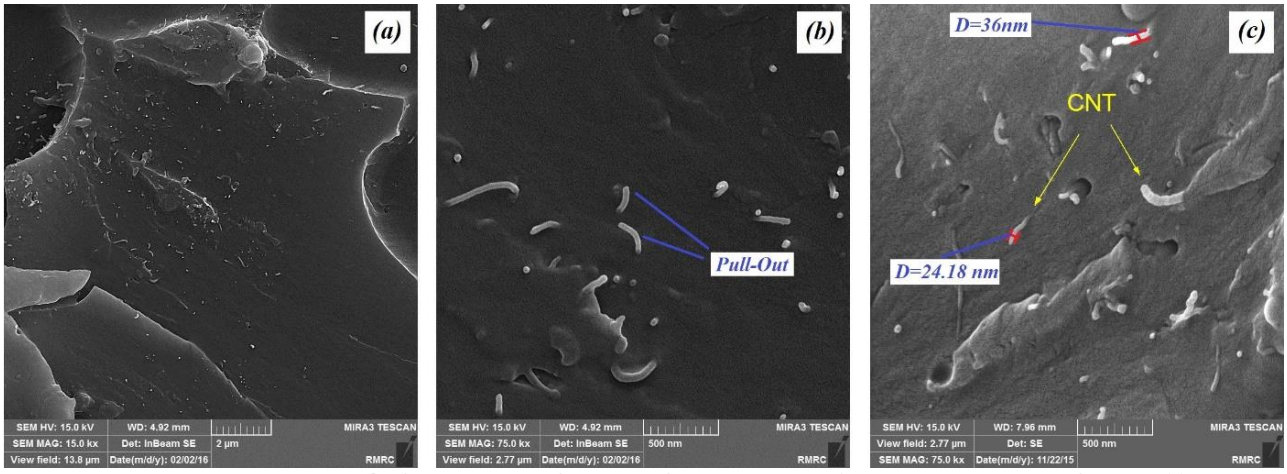

Figure 6. FESEM micrograph of nanocomposite fracture surface containing 0.45 wt. % MWCNTs at magnifications: (a) 15,000x, (b) 75,000x, and (c) 75,000x

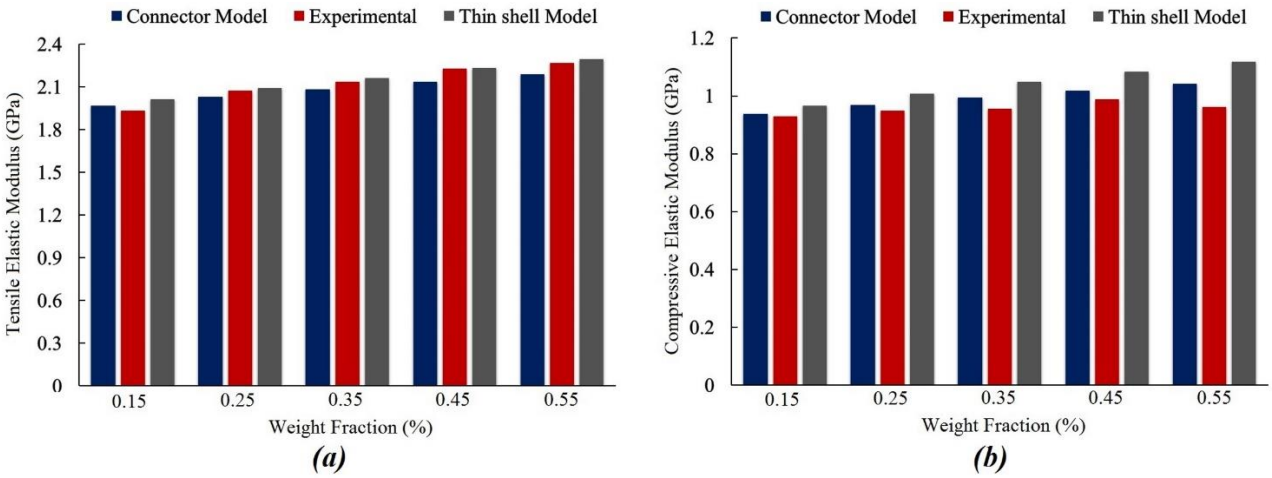

Figure 7. Comparison of modulus of elasticity determined numerically with experimental measurements

Next our numerical results are compared with available experimental results to evaluate the validity of our models. For this comparison, the data presented by Montazeri et al. [10] is used. Montazeri et al. [10] presented experimental results for seven different samples with 0, 0.1, 0.5, 1.0, 1.5, 2.0, and 3.0 nanotube weight fractions. This comparison is presented in Fig. 8. It can be seen in this figure that our results are in excellent agreement with the results presented by Montazeri et al. [10]. The difference between the results of the current investigation and the reference results is less than 17% for high MWCNT weight fraction.

4.4. Numerical Simulation Results

After validating the numerical simulation results, the effects of interphase stiffness on mechanical properties of MWCNT reinforced epoxy resin were investigated through a series of numerical simulations. The two effective Young's moduli (E_z, E_x) are determined using finite element method. Because of the symmetry of the reinforced RVE, a quarter of the RVE was modeled in Abaqus. The boundary conditions and loadings were applied to the models as discussed above.

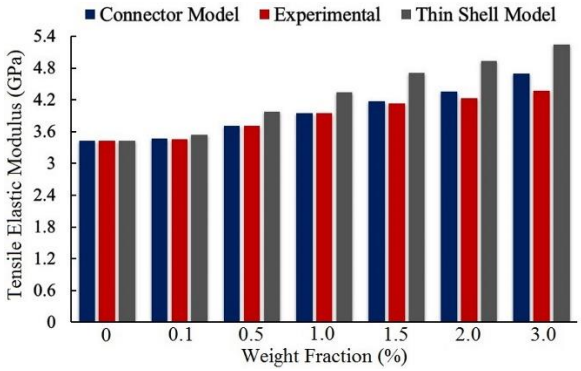

Figure 8. Comparison of the results of current investigation with experimental results presented by Montazeri et. al [10]

In these simulations, to investigate the effects of the interface strength on nanocomposite mechanical properties, two models were used. According to the weak nature of van der Waals bonds, the interface strength was assumed to be lower than the matrix strength. These models and the corresponding results are discussed in the next sections.

4.4.1. Connector Constraint Interface

In the first model, connector constraints were used as an interface between the carbon nanotube layers as well as the matrix/CNT interface. Axial loads on the RVE result in relative movement of the CNT layers. This relative movement results in a shear force build-up on the surfaces of the individual CNT tubes and on the CNT/matrix interface. This shear force then results in a moment about the *x*-axis, as shown in Fig. 3, and affects the stress transfer between nanotube layers, and at the CNT/matrix interface. To account for this phenomenon, hinge-type connectors were used. These connectors support only the torsional degree of freedom about the *x*-axis (UR1).

Lateral loads result in the relative stretching/contraction of the CNT layers in the transverse direction. To account for the resulting stresses for this load case, radial link elements were used in these regions. The coordinate axes of these link elements were set to follow the loading direction along the CNT perimeter. This results in pure elongation of the connectors which are aligned along the transverse loading direction. The same is true for the connectors aligned perpendicular to the loading direction (i.e. pure contraction). The connectors that align in between those orientations support both axial and torsional loads.

The interface strength strongly affects the nanocomposite mechanical properties. However, the exact bonding strength in the interface region is unknown due to different parameters involved. To account for the interface strength effect, axial and

torsional stiffness of tested connectors were varied from 0.2 to 1.89 GPa in nine steps. A sample stress contour plot of the RVE is shown in Fig. 9. The maximum stress is observed to occur at the CNT/matrix interface. Also, the stresses decrease moving radially in toward the inner CNT layer. The FE results investigating the interface effect on nanocomposite Young's moduli are shown in Fig. 10. Note that the nanocomposite moduli of elasticity have been normalized with matrix modulus of elasticity (E_m).

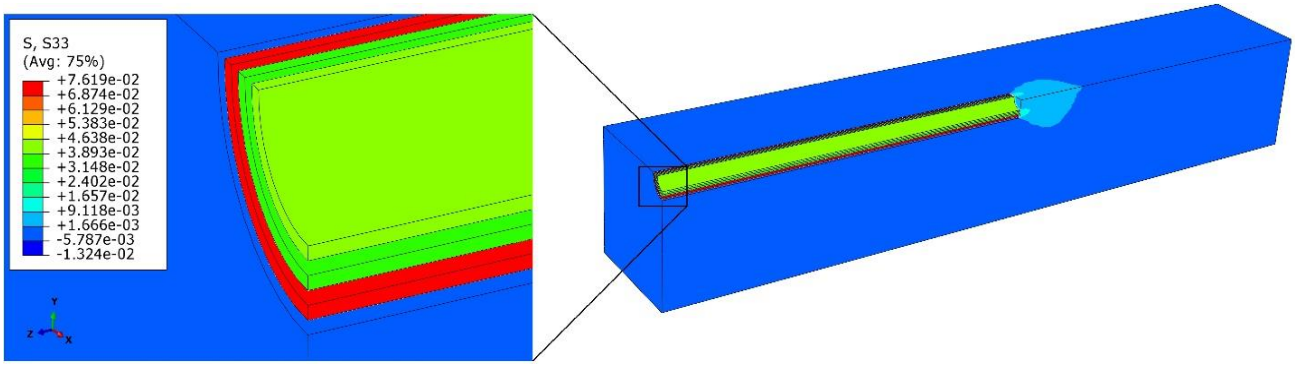

Figure 9. Magnification plot of stress distribution in the model with connector constraint interface

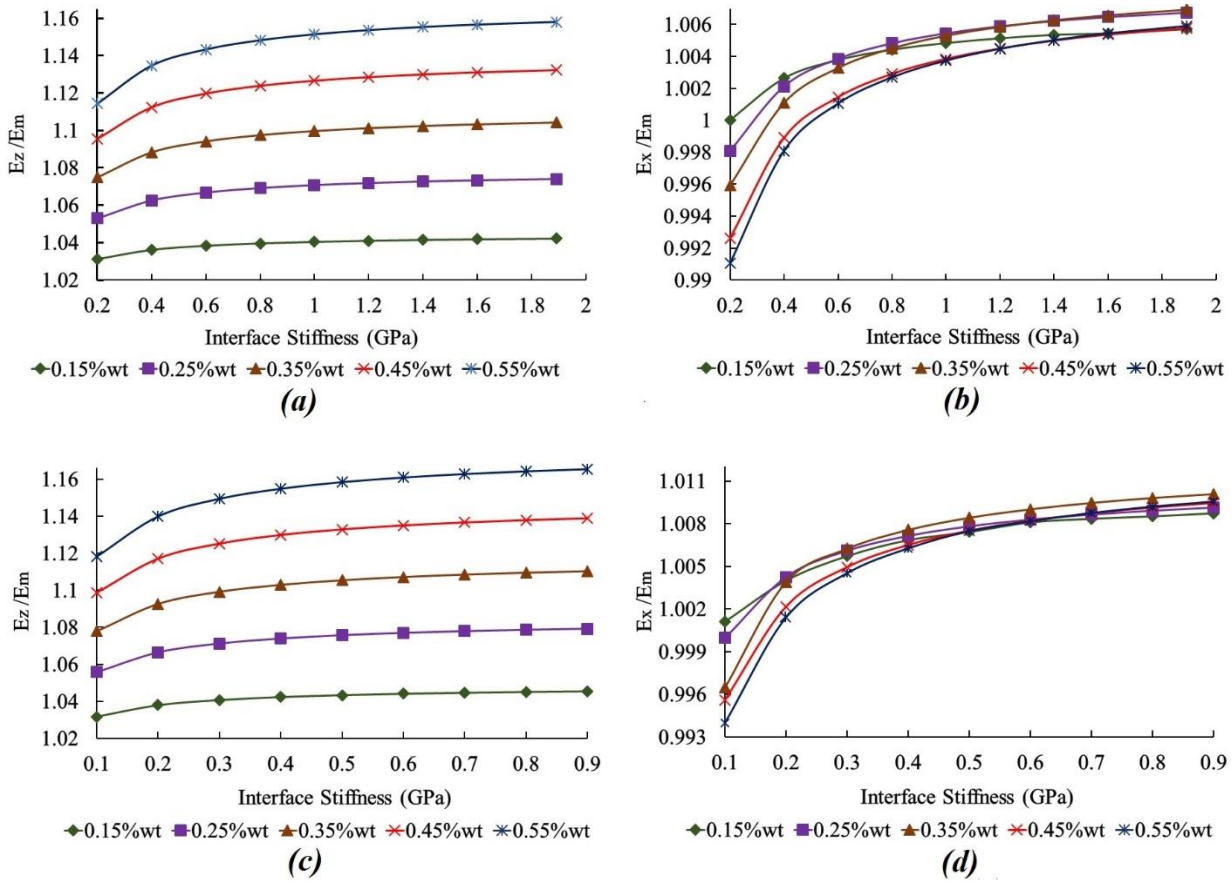

Figure 10. Variation of nanocomposite mechanical properties with connector constraints stiffness for various MWCNTs weight fractions: (a) variation of E_z/E_m (tensile), (b) variation of E_x/E_m (tensile), (c) variation of E_z/E_m (compression), (d) variation of E_x/E_m (compression)

4.4.2. Thin shell interface

In the second set of models, an interface consisting of a thin shell was considered around individual CNT layers in the MWCNTs. The interface strength was varied in nine steps between 0.2 to 1.89 GPa (perfect bonding). An example of a stress distribution plot of this model is shown in Fig. 11. A comparison between these results with those obtained using the connector constraints, suggests that stress transfer is higher in the thin shell interface model. Variation of nanocomposite Young's moduli with interface strength is shown in Fig. 12 for this case.

As shown in this figure, nanocomposite longitudinal modulus increases with the interface strength. Interface strength, however, has little effect on nanocomposite transverse modulus. Note in Figs. 10 and 12 that the results approximately converge to constant values at interface strength of 1.2 GPa. This value was therefore used in the numerical simulations.

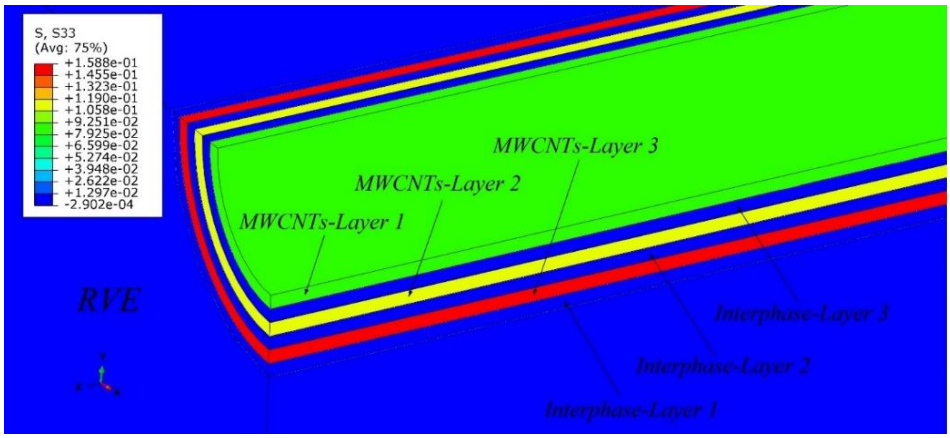

Figure 11. Magnification plot of stress distribution in thin shell interface model

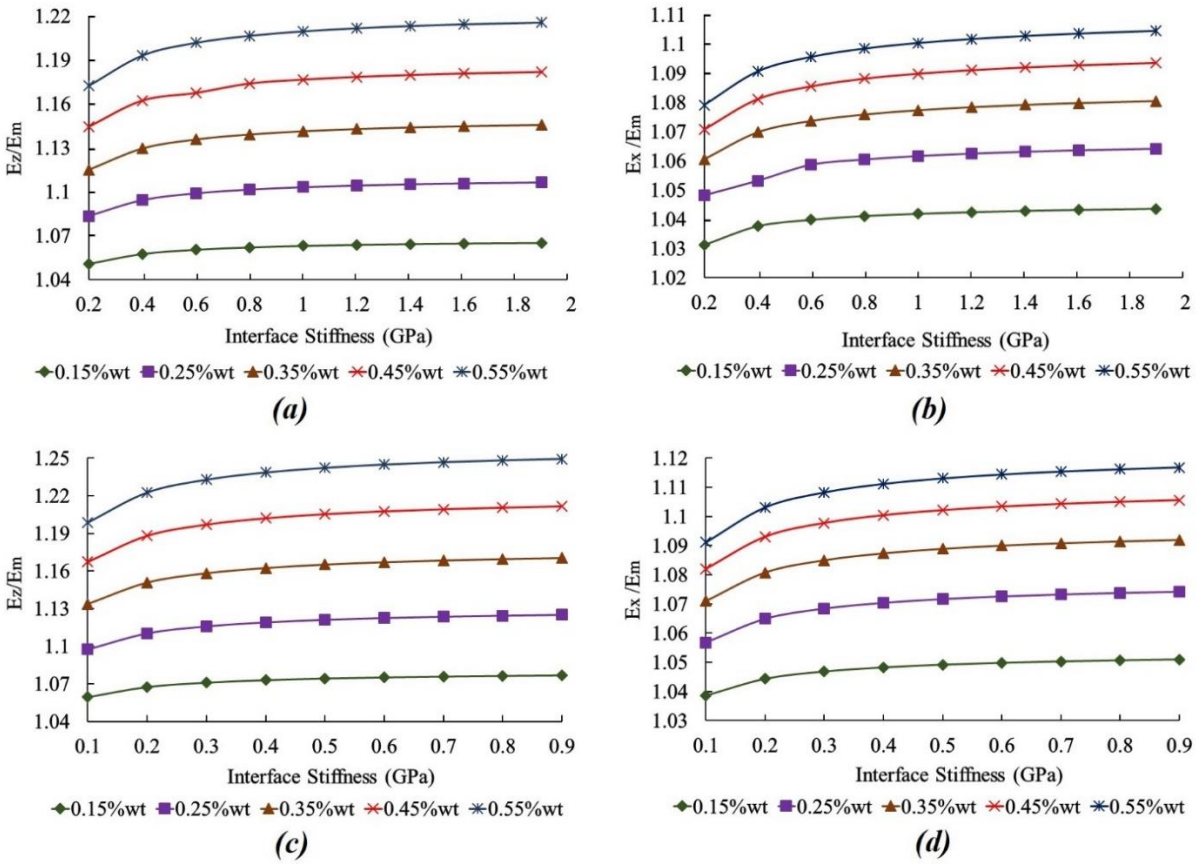

Figure 12. Variation of nanocomposite mechanical properties with thin shell stiffness for various MWCNTs weight fractions: (a) variation of E_z/E_m (tensile), (b) variation of E_x/E_m (tensile), (c) variation of E_z/E_m (compression), (d) variation of E_x/E_m (compression)

5. Conclusions

In this study, experimental tests were performed to determine tensile and compressive behaviors of Multi-Walled Carbon Nanotube reinforced epoxy resin. Samples containing 0.0, 0.15, 0.25, 0.35, 0.45 and 0.55 CNT weight percent were prepared and tested under tensile and compessive loading. Experimental results indicate a meaningful increase in resin modulus of elasticity, yield strength, and ultimate strength with CNT weight fraction. However, tensile fracture strain shows a significant decrease with CNT weight fraction. In addition, Field Emis-

sion Scanning Electron Microscope (FESEM) was used to observe fracture surfaces and MWCNTs dispersion in epoxy resin. These images prove good CNT dispersion in the matrix. Fiber pull-out is observed in the micrographs. Numerical simulations were also performed to estimate the mechanical properties of multi-walled carbon nanotube reinforced epoxy resin. The effects of imperfect bonding at the CNT/matrix interface were accounted for in numerical models. For this purpose, two different models are presented. These interface models are connector constraint interface and thin shell interface. The comparison between numerical results and experimental measurements indicate less than 5% error. The results also indicate that the thin shell interface model gives a better prediction of nanocomposite modulus of elasticity. The results of connector constraint models are compared with experimental results presented in the references and good agreement is observed.

References

[1] Alian AR, El-Borgi S, Meguid SA. Multiscale Modeling of the Effect of Waviness and Agglomeration of CNTs on the Elastic Properties of Nanocomposites. *Comput Mater Sci* 2016; 117: 195-204.

[2] Joshi UA, Sharma SC, Harsha SP. Effect of Carbon Nanotube Orientation on the Mechanical Properties of Nanocomposites. *Compos. B* 2012; 43: 2063-2071.

[3] Alian AR, Kundalwal SI, Meguid SA. Multiscale Modeling of Carbon Nanotube Epoxy Composites. *Polym* 2015; 70: 149-160.

[4] Banerjee D, Nguyen T, Chuang TJ. Mechanical Properties of Single-walled Carbon Nanotube Reinforced Polymer Composites with Varied Interphase's Modulus and Thickness: A Finite Element Analysis study. *Comput Mater Sci* 2016; 114: 209-218.

[5] Gkikas G, Barkoula NM, Paipetis AS. Effect of Dispersion Conditions on the Thermo-Mechanical and Toughness Properties of Multi Walled Carbon Nanotubes Reinforced Epoxy. *Compos B* 2012; 43: 2697-2705.

[6] Alval A, Bhagat A, Raja S. Effective Moduli Evaluation of Carbon Nanotube Reinforced Polymers Using Micromechanics. *Mech Adv Mater Struct* 2015; 22: 819-828.

[7] Srivastava VK. Modeling and Mechanical Performance of Carbon Nanotube/Epoxy Resin Composites. *Mater Des* 2012; 39: 432-436.

[8] Yas MH, Mohammadi S, Astinchap B, Heshmati M. A Comprehensive Study on the Thermo-Mechanical Properties of Multi-Walled Carbon Nanotube/Epoxy Nanocomposites. *J Compos Mater* 2015; 0: 1-10.

[9] Rahmanian S, Suraya AR, Shazed MA, Zahari R, Zainudin ES. Mechanical Characterization of Epoxy Composite with Multiscale Reinforcements: Carbon Nanotubes and Short Carbon Fibers. *Mater Des* 2014; 60: 34-40.

[10] Montazeri A, Javadpour J, Khavandi A, Tcharkhtchi A, Mohajeri A. Mechanical Properties of Multi-Walled Carbon Nanotube/Epoxy Composites. *Mater Des* 2010; 31: 4202-4208.

[11] Ayatollahi MR, Shadlou S, Shokrieh MM, Chitsazzadeh M. Effect of Multi-Walled Carbon Nanotube Aspect Ratio on Mechanical and Electrical Properties of Epoxy-Based Nanocomposites. *Polym Testing* 2011; 30: 548-556.

[12] Xu LR, Bhamidipati V, Zhong WH, Li J, Lukehart CM. Mechanical Property Characterization of a Polymeric Nanocomposite Reinforced by Graphitic Nanofibers with Reactive Linkers. *J Compos Mater* 2004; 38: 1563-1582.

[13] Fereidoon A, Rostamiyan Y, Omrani A, Kordani N, Ganji DD. Statistical Study on Nonlinear Effect of Carbon Nanotube on Mechanical Properties of Epoxy Composite. *J Compos Mater* 2011; 46(7): 861-868.

[14] Maa PC, Siddiqui NA, Marom G, Kim JK. Dispersion and Functionalization of Carbon Nanotubes for Polymer-Based Nanocomposites. *Compos A Rev* 2010; 41: 1345-1367.

[15] Montazeri A, Chitsazzadeh M. Effect of Sonication Parameters on the Mechanical Properties of Multi-Walled Carbon Nanotube/Epoxy Composites. *Mater Des* 2014; 56: 500-508.

[16] Chen ZK, Yang JP, Ni QQ, Fu SY, Huang YG. Reinforcement of Epoxy Resins with Multi-Walled Carbon Nanotubes for Enhancing Cryogenic Mechanical Properties. *Polym* 2009; 50: 4753-4759.

[17] Ma P, Jiang G, Chen Q, Cong H, Nie X. Experimental Investigation on the Compression Behaviors of Epoxy with Carbon Nanotube under High Strain Rates. *Compos B* 2015; 69: 526-533.

[18] Ghosh PK. Kumar K, Chaudhary N. Influence of Ultrasonic Dual Mixing on Thermal and Tensile Properties of MWCNTs-Epoxy Composite. *Compos B* 2015; 77: 139-144.

[19] Joshi P, Upadhyay SH. Evaluation of Elastic Properties of Multi Walled Carbon Nanotube Reinforced Composite. *Comput Mater Sci* 2014; 81: 332-338.

[20] Joshi P, Upadhyay SH. Effect of Interphase on Elastic Behavior of Multi Walled Carbon Nanotube Reinforced Composite. *Comput Mater Sci* 2014; 87: 267-273.

[21] Giannopoulos GI, Georgantzinos SK, Anifantis NK. A Semi-Continuum Finite Element Approach to Evaluate the Young's Modulus of Single-Walled Carbon Nanotube Reinforced Composites. *Compos B* 2010; 41: 594-601.

[22] Weidt D, Figiel L. Finite Strain Compressive Behaviour of CNT/Epoxy Nanocomposites: 2D ver-

sus 3D RVE-Based Modeling. *Comput Mater Sci* 2014; 82, 298-309.
[23] Zuberi MJS, Esat V. Investigating the Mechanical Properties of Single Walled Carbon Nanotube Reinforced Epoxy Composite Through Finite Element Modeling. *Compos B* 2015; 71: 1-9.
[24] Shokrieh MM, Rafiee R. Investigation of Nanotube Length Effect on the Reinforcement Efficiency in Carbon Nanotube Based Composites. *Compos Struct* 2010; 92: 2415-2420.
[25] Mohammadpour E, Awang M, Kakooei S, Akil HM. Modeling the Tensile Stress Strain Response of Carbon Nanotube/Polypropylene Nanocomposites Using Nonlinear Representative Volume Element. *Mater Des* 2014; 58: 36-42.
[26] Golestanian H, Shojaie M. Numerical Characterization of CNT-Based Polymer Composites Considering Interface Effects. *Comput Mater Sci* 2010; 50: 731-736.
[27] Bakhtiar NSAA, Akil HMD, Zakaria MR, Kudus MHA, Othman MBH. New Generation of Hybrid Filler for Producing Epoxy Nanocomposites with Improved Mechanical Properties. *Mater Des* 2016; 91: 46-52.
[28] ASTM D638-99, Standard test method for tensile properties of plastics, West Conshohocken, PA: ASTM International, www.astm.org; 2010.
[29] ASTM D695-10. Standard test method for compressive properties of plastics. West Conshohocken, PA: ASTM International, www.astm.org; 2010.
[30] Ghahfarokhi ZM, Golestanian H. Effects of Nanotube Helical Angle on Mechanical Properties of Carbon Nanotube Reinforced Polymer Composites. *Comput Mater Sci* 2011; 50: 3171-3177.